Elastostatic fields in an anisotropic substrate due to a buried quantum dot

E. Pan[a] and B. Yang
Structures Technology Inc., 543 Keisler Drive, Suite 204, Cary, North Carolina 27511

(Received 23 July 2001; accepted for publication 7 September 2001)

We present an efficient and accurate continuum-mechanics approach for the numerical prediction of displacement, stress, strain, and strain energy density fields in an anisotropic substrate (modeled as a half-space) due to a buried quantum dot (QD). Our approach is based on Green's function solution in anisotropic and linearly elastic half-space combined with the Betti's reciprocal theorem. Numerical examples clearly show that the crystalline anisotropy of the III–V semiconductor group has great influence on the elastic fields, as compared to the isotropic solution. In particular, it is found that the hydrostatic strain and strain energy density on the surface of anisotropic half-space made of different crystalline materials due to a cubic QD can be substantially different, and therefore, the isotropy approximation neglecting their differences should not be used in general. Furthermore, the hydrostatic strains on the surface of an anisotropic half-space due to a finite-size (cubic) QD and an equal-intensity point QD at relatively large depth (about twice the side length of the cubic QD) can still be quite different, in contrast to the corresponding isotropic result. These observations indicate that in modeling and analyzing the mechanical and electronic behaviors of QD semiconductor structures, the effect of crystalline anisotropy should be considered in general. [DOI: 10.1063/1.1415542]

I. INTRODUCTION

Recent experimental studies on self-assembled quantum dot (QD) semiconductor structures have shown that such structures possess certain special electronic and optical features, rendering possible fascinating novel devices.[1] To quantitatively explain and numerically model the QD structures, various numerical methods have been proposed, including the finite element method (FEM) and finite difference method (FDM).[2–4] However, the domain-based FEM and FDM are computationally expensive, making them difficult to perform parametric studies in order to understand the experimental phenomena or to reach an economic design strategy.

In recent years, various analytical methods, in particular those related to the Green's function solutions have been proposed and applied to the QD modeling.[5,6] Because of their robust features in terms of accuracy and efficiency, these analytical methods, particularly the Green's function method, have been found to be very useful in the studies of QD structures.[5–10] For QDs in a three-dimensional (3D) isotropic infinite space, Pearson and Faux[10] derived an exact-closed form solution for the QD-induced strain when the QDs are in the form of a pyramid. When the infinite domain is anisotropic, Andreev *et al.*[9] and Faux and Pearson[6] derived the induced strain using, respectively, the Fourier transform method and series expansion method, with the latter being advanced from previous solutions.[11–14] As is well known, however, a semiconductor structure is better modeled with an anisotropic half-space or an anisotropic multilayered model. Unfortunately, the existence of a free surface combined with material anisotropy substantially complicates the Green's function problem, and thus the analytical Green's function solutions have been long restricted to the isotropic or transversely isotropic half space.[15–19] Therefore to solve the related problems only the computationally expensive method, either the Fourier transform method or the domain-discretization method (FEM or FDM) was used. For example, assuming a buried point misfit strain in an anisotropic half-space, Holy *et al.*[20] using the Fourier transform method solved the strain energy density in various semiconductors and found that the superlattice orientation and direction are closely correlated with the material anisotropy. On the other hand, assuming an isotropic half space and using the FEM method, Romanov *et al.*[19] studied the effect of the finite-size QD on the elastic field and observed that the geometrical shape and size of the QDs can have a great influence on the hydrostatic pressure and volumetric strain fields. We further mention that Grundmann *et al.*[2] simulated numerically a pyramidal InAs/GaAs QD on a thin wetting layer using the FDM method and found various interesting results related to the strain distribution, optical phonons, and electronic structure.

Very recently, the point-force Green's functions in a generally anisotropic elastic half-space were derived by Pan and Yuan[21] based on the extended Stroh formalism, which is both mathematically elegant and numerically powerful.[22] The Green's functions are expressed as a sum of an infinite-space Green's function and a complementary part. While the former can be evaluated in an explicit analytical form,[23] the latter is expressed in terms of a regular line integral over $[0,\pi]$ that resembles the Mindlin's complementary solution.[15] The reduction of the integral dimension by one in the complementary part significantly reduces the effort in computing the physical half-space Green's functions.

In this article these recently derived 3D Green's functions in anisotropic half-spaces are applied to the study of the elastostatic fields in an anisotropic half-space due to an em-

[a]Electronic mail: ernian_pan@yahoo.com

bedded QD. Using the Betti's reciprocal theorem, the QD-induced elastic fields are expressed in terms of a simple integral over the surface of the QD with the point-force Green's functions as the kernels. Furthermore, if the QD is a point source, then the QD-induced elastic fields can be analytically expressed by the point-force Green's functions in the anisotropic half-space. These novel features make them easy to perform accurate and efficient parametric studies in analyzing and designing the semiconductor structures. Numerical examples are carried out for a buried cubic QD in anisotropic half-spaces made of the III–V semiconductors, and the following important features are observed: (1) Crystalline anisotropy of the III–V semiconductors (with degrees of anisotropy varying from -0.3 to -0.5) has a great influence on the QD-induced hydrostatic strain and strain energy density. Since these quantities are directly related to the electronic properties of semiconductor QD structures, the effect of anisotropy should be considered when analyzing and designing these structures. In particular, the simplified isotropic structure should not be used if the structure shows clear anisotropy. (2) In anisotropic semiconductors the effect of the QD shape can still be significant even if the QD is buried at a relatively deep location. This is in contrast to the well-known observation on the corresponding isotropic half-space that when a 3D QD with a characteristic length a located at the depth $2a$ or larger, the induced surface strain due to the finite-size and an equal-intensity point QDs are then very close to each other.[19] Therefore one needs to be extra cautious when approximating a finite-size QD with an equal-intensity point QD.

II. Theory

The misfit-strain problem in an anisotropic and linearly elastic half-space can be described in terms of an integral-equation formulation with integral kernels being the point-force Green's functions in the same half-space. This integral formulation is a consequence of the Betti's reciprocal theorem. Assume two states associated with the half space: One for the misfit-strain problem due to a misfit strain ϵ^*_{ij} in a finite subdomain Ω of the half-space D, and another for the Green's solution due to a point force. Then the displacement $u_k(\mathbf{y})$ due to the misfit strain ϵ^*_{ij} can be expressed by the following integral equation as

$$u_k(\mathbf{y}) = \int_{\partial D} [u_i^k(\mathbf{x};\mathbf{y})\sigma_{ij}(\mathbf{x})n_j(\mathbf{x}) - \sigma_{ij}^k(\mathbf{x};\mathbf{y})n_j(\mathbf{x})u_i(\mathbf{x})]dS(\mathbf{x}) + \int_D u_i^k(\mathbf{x};\mathbf{y})[-C_{ijlm}\epsilon^*_{lm,j}(\mathbf{x})]dV(\mathbf{x}), \quad (1)$$

where ∂D is the boundary of D (i.e., the surface of the half-space) and $u_i^k(\mathbf{x};\mathbf{y})$ and $\sigma_{ij}^k(\mathbf{x};\mathbf{y})$ are the Green's ith displacement and ijth stress components at $\mathbf{x}$ due to a point force in the kth direction applied at $\mathbf{y}$. Recently, Pan and Yuan[21] derived the half-space Green's functions for the traction-free surface condition and Pan[24] for the general surface condition, both using the extended Stroh formalism[22] and the Mindlin's superposition method.[15] These Green's functions, along with their derivatives with respect to the source coordinate $\mathbf{y}$, are summarized in the Appendix for the sake of convenient reference.

TABLE I. Elastic constants of some III–V semiconductors (10^{11} Pa).

	C_{11}	C_{12}	C_{22}	C_{an}
GaAs	1.18	0.54	0.59	−0.54
InAs	0.83	0.45	0.40	−0.42
GaSb	0.88	0.40	0.43	−0.38
InSb	0.66	0.36	0.30	−0.30
Isotropy	1.72	0.54	0.59	0.00

Since the misfit strain ϵ^*_{ij} is applied only in the finite subdomain Ω of D and the surface of the half-space is traction-free, it is evident that the integration on the boundary ∂D in Eq. (1) is zero. Therefore Eq. (1) is reduced to[16]

$$u_k(\mathbf{y}) = \int_D u_i^k(\mathbf{x};\mathbf{y})[-C_{ijlm}\epsilon^*_{m}(\mathbf{x})_{,j}]dV(\mathbf{x}). \quad (2)$$

Shifting the differentiation in Eq. (2) by applying the Gauss theorem we obtain

$$u_k(\mathbf{y}) = \int_\Omega C_{ijlm}u^k_{i,x_j}(\mathbf{x};\mathbf{y})\epsilon^*_{lm}(\mathbf{x})dV(\mathbf{x}). \quad (3)$$

In Eq. (3) the domain-integral has been reduced from D to Ω due to the fact that the misfit strain is nonzero in Ω only. Furthermore, the domain-integral in Eq. (3) can be reduced to the surface of Ω if the misfit strain is uniform in Ω. That is

$$u_k(\mathbf{y}) = C_{ijlm}\epsilon^*_{lm}\int_{\partial\Omega} u_i^k(\mathbf{x};\mathbf{y})n_j(\mathbf{x})dS(\mathbf{x}), \quad (4)$$

where $n_j(\mathbf{x})$ are the outward normal components on the surface of Ω.

In order to find the total strain field we take the derivatives of Eq. (4) with respect to the observation point $\mathbf{y}$ (i.e., the source point for the point-force Green's functions), which yields

$$\epsilon_{kp}(\mathbf{y}) = \tfrac{1}{2}\epsilon^*_{lm}\int_{\partial\Omega} C_{ijlm}[u^k_{i,y_p}(\mathbf{x};\mathbf{y}) + u^p_{i,y_k}(\mathbf{x};\mathbf{y})]n_j(\mathbf{x})dS(\mathbf{x}). \quad (5)$$

The corresponding stress field is thus obtained by

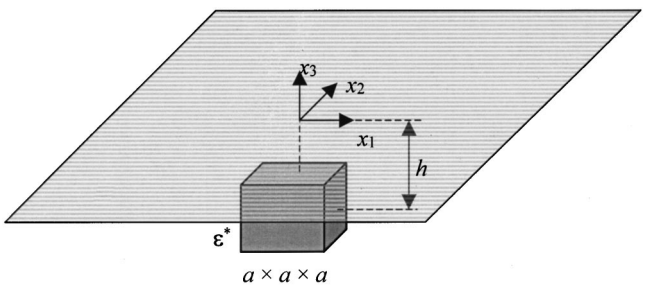

FIG. 1. A buried cubic QD of size $a\times a\times a$ with its center at a depth of h below the traction-free surface of a half-space.

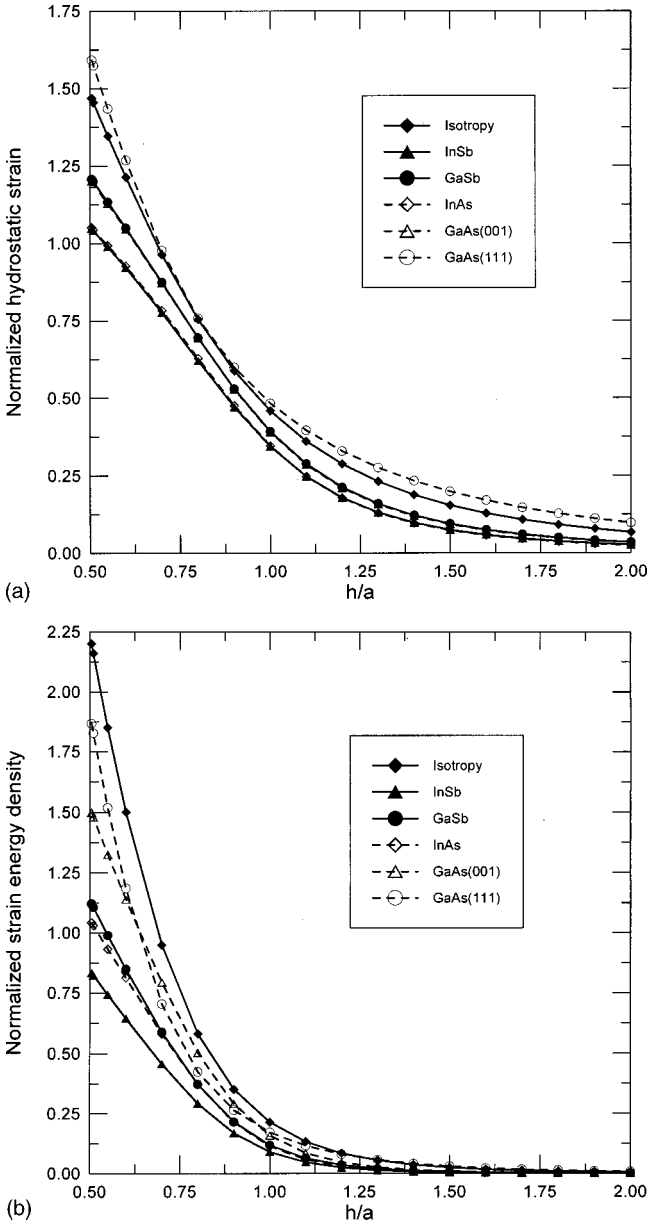

FIG. 2. (a) Variation of the normalized hydrostatic strain ϵ_{kk}/ϵ^* on the surface of the half space at $\mathbf{x}=(0,0,0)$ with the normalized QD depth h/a, for isotropic and anisotropic crystals. (b) Variation of the normalized strain energy density $0.5C_{ijkl}\epsilon_{ij}\epsilon_{kl}/(C_0\epsilon^*)$ on the surface of the half space at $\mathbf{x}=(0,0,0)$ with the normalized QD depth h/a, for isotropic and anisotropic crystals ($C_0=10^{11}$ Pa).

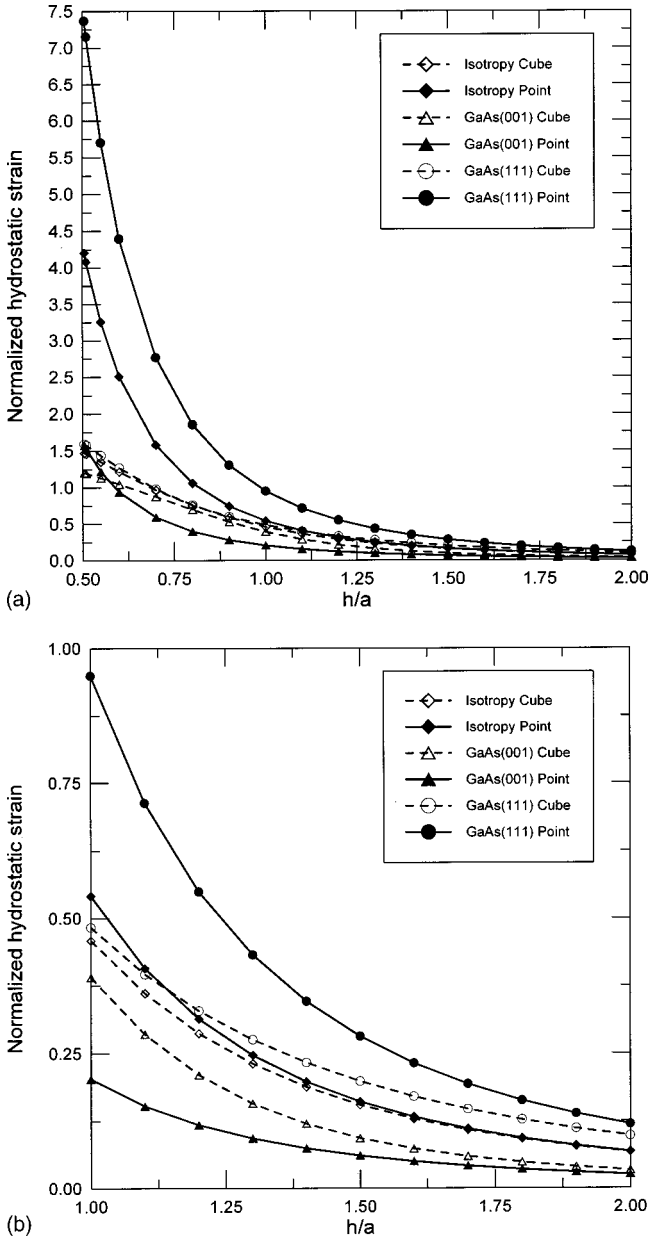

FIG. 3. (a) Comparison of the variation of the normalized hydrostatic strain ϵ_{kk}/ϵ^* on the surface of the half-space at $\mathbf{x}=(0,0,0)$ with the normalized QD depth h/a due to a cubic QD and a point QD, for both isotropic and anisotropic crystals. (b) Same as in (a) but for the zoom-in result.

$$\sigma_{ij}(\mathbf{y})=C_{ijkp}[\epsilon_{kp}(\mathbf{y})-\chi\epsilon^*_{kp}], \tag{6}$$

where χ equals 1 if the observation point $\mathbf{y}$ is within the misfit-strain domain Ω, and 0 otherwise.

With the strain and stress fields being given by Eqs. (5) and (6), respectively, the corresponding strain energy density w at the point $\mathbf{y}$ can be evaluated using the following expression

$$w(\mathbf{y})=\tfrac{1}{2}\sigma_{ij}(\mathbf{y})\epsilon_{ij}(\mathbf{y}). \tag{7}$$

Finally, for a point misfit strain applied at point $\mathbf{x}_0$, i.e., $\epsilon^*_{lm}\delta(\mathbf{x}-\mathbf{x}_0)$, the induced displacement and strain fields can be expressed directly by the point-force Green's functions with neither volumetric nor surface integration. That is, the induced displacement and strain fields by the point misfit strain are analytically found to be, respectively,

$$u_k(\mathbf{y})=\sigma^k_{lm}(\mathbf{x}_0;\mathbf{y})\epsilon^*_{lm} \tag{8}$$

and

$$\epsilon_{kp}(\mathbf{y})=\tfrac{1}{2}\epsilon^*_{lm}[\sigma^k_{lm,y_p}(\mathbf{x}_0;\mathbf{y})+\sigma^p_{lm,y_k}(\mathbf{x}_0;\mathbf{y})]. \tag{9}$$

It is observed from Eq. (8) that the displacement field in the kth direction at $\mathbf{y}$ due to a point misfit strain with components (lm) at $\mathbf{x}_0$ is equivalent to the stress field with components (lm) at $\mathbf{x}_0$ due to a point force in the kth direction at $\mathbf{y}$. We remark that while a similar observation can be made for Eq. (9), this equivalence, between a point force and a

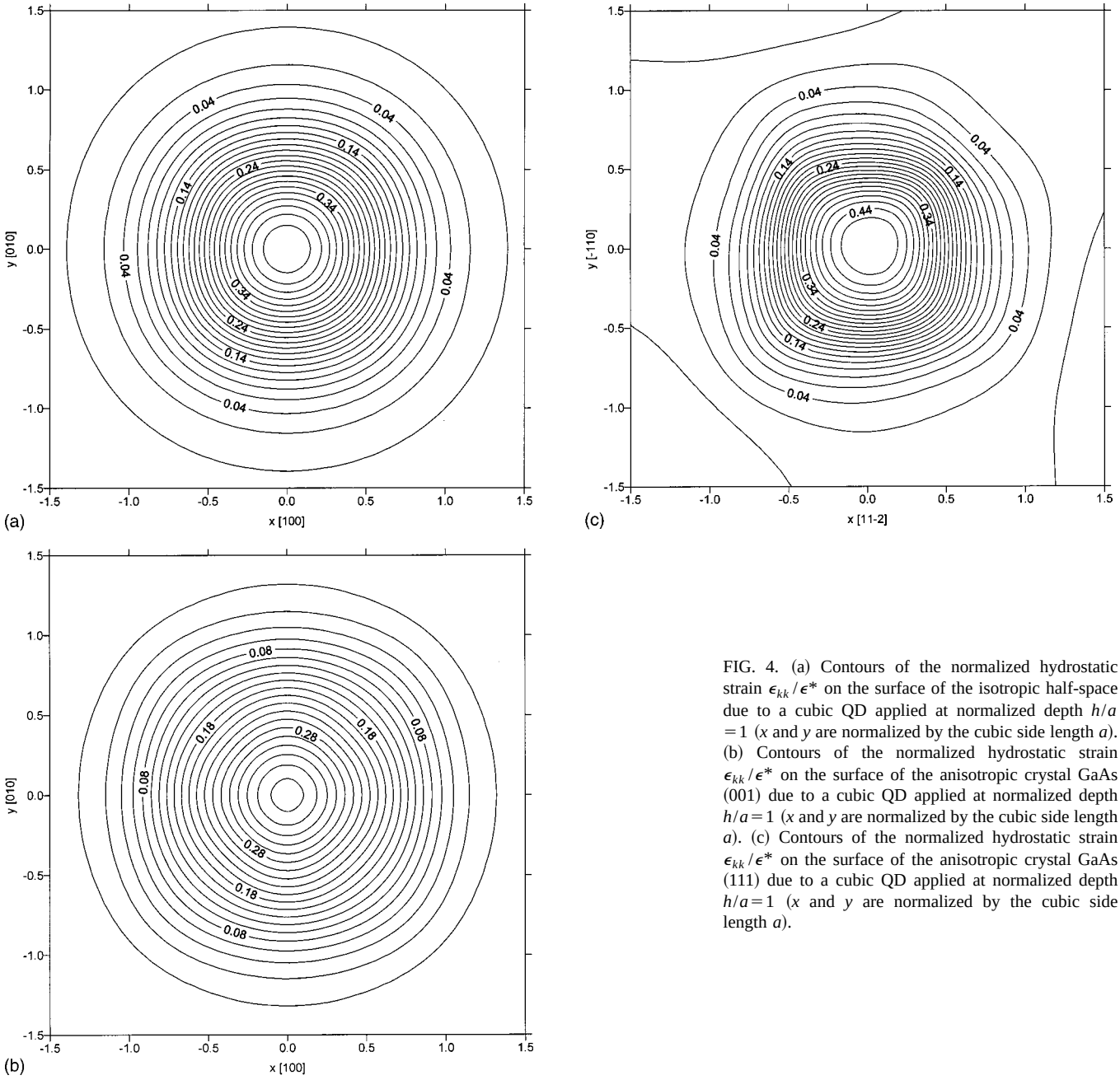

FIG. 4. (a) Contours of the normalized hydrostatic strain ϵ_{kk}/ϵ^* on the surface of the isotropic half-space due to a cubic QD applied at normalized depth $h/a=1$ (x and y are normalized by the cubic side length a). (b) Contours of the normalized hydrostatic strain ϵ_{kk}/ϵ^* on the surface of the anisotropic crystal GaAs (001) due to a cubic QD applied at normalized depth $h/a=1$ (x and y are normalized by the cubic side length a). (c) Contours of the normalized hydrostatic strain ϵ_{kk}/ϵ^* on the surface of the anisotropic crystal GaAs (111) due to a cubic QD applied at normalized depth $h/a=1$ (x and y are normalized by the cubic side length a).

point misfit strain, resembles the more general equivalence between a point force and a point dislocation solution.[25]

We further point out that the simple and analytical solutions developed in this section are based on the assumption that the elastic constants of the QD and matrix are the same. Otherwise (i.e., for the case where the elastic constants of the QD and matrix are different), one may need to use other advanced methods, such as the equivalent inclusion method explained in detail in the text of Mura[16] or the boundary integral equation method.[26,27]

III. RESULTS

Listed in Table I are the elastic constants for some III–V semiconductors used in this study for the substrate (half-space).[9,28] The last row in Table I is for an isotropic material reduced from GaAs by assuming that C_{12} and C_{44} are those of GaAs, but C_{11} is obtained using the isotropic relation. The parameter $C_{\text{an}}=C_{11}-C_{12}-2C_{44}$ is used to characterize the degree of anisotropy of the crystalline materials. We remark that, in the following calculation, the elastic constants are all normalized by $C_0=10^{11}$ Pa. Let us now assume that a cubic QD with a side length a is located at a depth h below the traction-free surface (Fig. 1), and that the misfit strain due to the mismatch lattice constants of the matrix (half-space) and the QD is hydrostatic within the QD material, i.e., $\epsilon_{ij}^*=\epsilon^*\delta_{ij}$. With the exception of the GaAs, all other crystals have their crystallographic axes along the half-space coordinates $(x_1,x_2,x_3)\equiv(x,y,z)$. In other words, the x, y, and z axes are, respectively, along the [100], [010], and [001] directions. For the GaAs, another crystal orientation with (111) being the surface of the half-space, denoted as GaAs (111) to distinguish GaAs (001) when (001) is the

surface of the half-space, is also studied. The other two axes in the GaAs (111) crystal are such that the x and y axes are along the [11-2] and [−110] directions, respectively.

Shown in Figs. 2(a) and 2(b) are the variations of the normalized hydrostatic strain ϵ_{kk}/ϵ^* and the normalized strain energy density $0.5C_{ijkl}\epsilon_{ij}\epsilon_{kl}/(C_0\epsilon^*)$ on the surface versus the normalized depth h/a, due to a cubic QD of size $a\times a\times a$. We remark that when $h/a=0.5$, the top surface of the cubic QD is then coincident with the surface of the half-space. It is observed clearly that crystal anisotropy has a great influence on both the hydrostatic strain and the strain energy density. For example, the largest and smallest (normalized) strain energy densities at $\mathbf{x}=(0,0,0)$, reached, respectively, in the isotropic material and InSb, are different by as large as three times in their magnitudes [Fig. 2(b)]. As for the hydrostatic strain, its largest and smallest values at $\mathbf{x}=(0,0,0)$ at any given depth are reached by GaAs (111) and InSb (InAs), respectively, with the isotropic material and GaSb [GaAs (001)] taking values between them [Fig. 2(a)]. While it is interesting that GaSb and GaAs (001), and InSb and InAs predict, respectively, nearly the same hydrostatic strain, the relative difference of the largest value by GaAs (111) and the smallest value by InSb, reached on the surface ($h/a=0.5$), is about 40%. We further emphasize that the effect of crystalline anisotropy does not vanish when the depth h increases. Actually, at $h/a=2.0$, we found that the difference of the largest and smallest hydrostatic strains is still as large as four times [Fig. 2(a)]. These great differences in the hydrostatic strain due to crystalline anisotropy will greatly influence the electronic energy gap between the valence and conduction bands since the latter is directly proportional to the former.[29,30]

Figure 3(a) shows the comparison of the variation of the normalized hydrostatic strain ϵ_{kk}/ϵ^* on the surface versus normalized depth h/a, due to a cubic QD of size $a\times a\times a$ with misfit strain $\epsilon^*\delta_{ij}$, and a point QD of equal intensity $a^3\epsilon^*\delta_{ij}\delta(\mathbf{x}-\mathbf{x}_0)$, where $\delta(\mathbf{x}-\mathbf{x}_0)$ is the Dirac delta function and $\mathbf{x}_0$ is the center of the cubic QD. The corresponding zoom-in result is plotted in Fig. 3(b). By selecting the three materials [the isotropic material, GaAs (001), and GaAs (111)], the purpose of these two figures is to show that when replacing a finite-size QD with an equal-intensity point QD, special care must be taken when the material is anisotropic. First, as we have observed before, the magnitudes of the hydrostatic strain induced by a QD in an isotropic and an anisotropic substrate can be greatly different. This feature can be clearly seen again from Figs. 3(a) and 3(b), where, for both cubic and point QD cases, the largest, intermediate, and smallest values are reached, respectively, in the GaAs (111), isotropic, and GaAs (001) half-spaces. Second, it is observed that with increasing depth h/a, the difference of the hydrostatic strains due to the cubic QD and point QD in the isotropic half-space becomes smaller and nearly vanishes when $h/a=2.0$, a result consistent with the observation made by Romanove *et al.*[19] However, when the half-space material is anisotropic, a point QD solution fails to approximate the finite-size QD solution at the same depth. For example, Fig. 3(b) shows that if the half-space is made of GaAs (111), then, when $h/a=2.0$, the difference of the hydrostatic strains

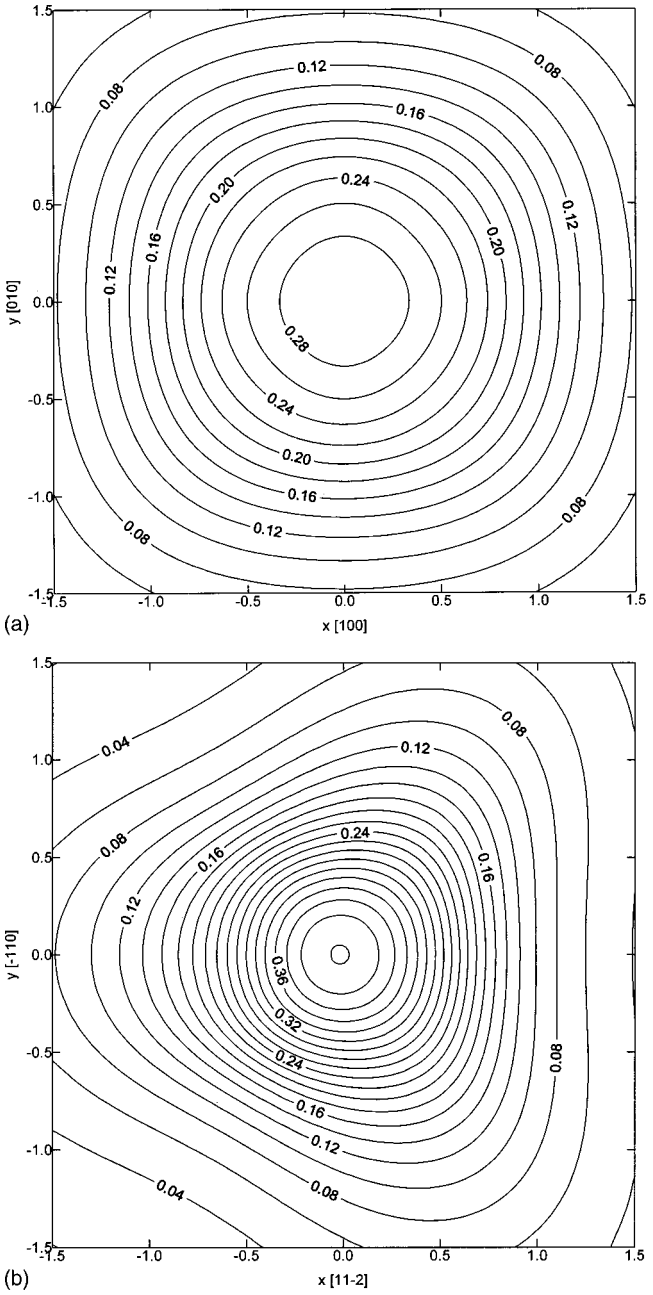

FIG. 5. (a) Contours of the normalized vertical displacement $u_z/(a\epsilon^*)$ on the surface of the anisotropic crystal GaAs (001) due to a cubic QD applied at normalized depth $h/a=1$ (x and y are normalized by the cubic side length a). (b) Contours of the normalized vertical displacement $u_z/(a\epsilon^*)$ on the surface of the anisotropic crystal GaAs (111) due to a cubic QD applied at normalized depth $h/a=1$ (x and y are normalized by the cubic side length a).

due to the cubic and point QDs can still be as large as 20%, large enough to affect the electronic band energies.

Shown in Figs. 4(a), 4(b), and 4(c) are, respectively, the surface contours of the hydrostatic strain in the isotropic, GaAs (001), and GaAs (111) half-spaces due to the cubic QD of size $a\times a\times a$ centered at the depth $h/a=1.0$. Besides the difference of their magnitudes, as we have observed before, their contour shapes are also different for different crystals. While the contour shapes in the isotropic crystal are nearly perfect circles, those in the anisotropic crystal are not, in

particular, in the GaAs (111) [Fig. 4(c)]. These differences can be observed more clearly by looking at the dimensionless vertical profiles $u_z/(\epsilon^* a)$ on the surface, as shown in Figs. 5(a) and 5(b) for GaAs (001) and GaAs (111), respectively. It is obvious that while the profile on the surface of GaAs (001) is a square-based pyramid, that on the surface of GaAs (111) is a triangle-based pyramid. We remark that Holy *et al.*[20] numerically predicted similar contour shapes for the strain energy density distributions, and correlated these contour shapes to the growth direction and orientation of the superlattice.

IV. CONCLUSIONS

In this article a recently derived 3D Green's function in an anisotropic half-space is applied to the study of elastic fields due to a QD embedded in a substrate. Using the Betti's reciprocal theorem, the QD-induced elastic fields are expressed in terms of a simple integral over the surface of the QD with the point-force Green's functions as the kernels. Furthermore, if the QD is a point source, then the QD-induced elastic field can be analytically expressed by the point-force Green's functions in the anisotropic half space. These features make the present continuum-mechanics approach easy to perform accurate and efficient parametric studies in analyzing and designing the semiconductor structures. Numerical examples are carried out for a buried cubic QD in an anisotropic half space made of the III–V semiconductors with the following important features being observed: (1) Crystal anisotropy has a great influence on the QD-induced hydrostatic strain and strain energy density. Since both the strain components and strain energy density are directly related to the electronic properties of the semiconductor QD structures, our studies have thus demonstrated that for a reliable numerical analysis on the semiconductor device, the simplified isotropic structure should not be used if the material clearly exhibits anisotropy. (2) Even if the buried QD is located at a relatively deep location, the effect of the QD shape may still be significant. This is in contrast to the well-known observation for the corresponding isotropic half-space that when a 3D QD with a characteristic length a is located at a depth $h=2a$ or larger, the induced surface strain due to a finite size and an equal-intensity point QD are very close to each other. Therefore, in the anisotropic structure, extra caution should be taken when approximating a finite size QD by an equal-intensity point QD.

ACKNOWLEDGMENTS

This work was supported partially by the AFOSR under Grant Nos. F33615-97-C-5089 and F33615-00-C-5503. The authors would like to thank the program manager Dr. Rick Hall for the support, and Professor C. Q. Ru of University of Alberta and Professor F. G. Yuan of North Carolina State University for their helpful comments.

APPENDIX

In this Appendix we briefly review the Green's functions in an anisotropic and linearly elastic half-space under a traction-free surface condition, with a detailed derivation in Pan and Yuan[21] and Pan.[24] The half-space Green's function is expressed as a sum of the full-space Green's function and a complementary part, which resemble the Mindlin's solution for the corresponding isotropic half-space.[15] While the full-space Green's function has been derived in an explicit analytical form,[23] the complementary part is expressed in terms of a regular line integral that can be easily evaluated by a standard quadrature scheme.

We first define the so-called extended Stroh eigenvalues and eigenmatrices.[22] The extended Stroh eigenvalue p_j and the eigenmatrice $\mathbf{A}=[\mathbf{a}_1,\mathbf{a}_2,\mathbf{a}_3]$ are the solutions of the following eigenrelation[21,22]

$$[\mathbf{Q}+p_j(\mathbf{R}+\mathbf{R}^T)+p^2\mathbf{T}]\mathbf{a}_j=0, \tag{A1}$$

where the superscript T denotes matrix transpose, and

$$Q_{ik}=C_{i\alpha k\beta}n_\alpha n_\beta, \quad R_{ik}=C_{i\alpha k3}n_a, \quad T_{ik}=C_{i3k3} \tag{A2}$$

with

$$(n_1,n_2)\equiv(\cos\theta,\sin\theta) \tag{A3}$$

and α and β taking the values of 1 and 2. We remark that, due to the positive requirement on the strain energy density, the eigenvalues of Eq. (A1) are either complex or purely imaginary.[22]

We then define the other two matrices $\mathbf{B}=[\mathbf{b}_1,\mathbf{b}_2,\mathbf{b}_3]$ and $\mathbf{C}=[\mathbf{c}_1,\mathbf{c}_2,\mathbf{c}_3]$ related to the Stroh eigenmatrix $\mathbf{A}$ as

$$\mathbf{b}_j=(\mathbf{R}^T+p_j\mathbf{T})a_j=-\frac{1}{p_j}(\mathbf{Q}+p_j\mathbf{R})\mathbf{a}_j,$$
$$\mathbf{c}_j=\mathbf{D}_j\mathbf{a}_j, \tag{A4}$$

where the matrix $\mathbf{D}_j$ is defined by

$$\mathbf{D}_j=\begin{bmatrix} C_{111\alpha}n_\alpha+p_jC_{1113} & C_{112\alpha}n_\alpha+p_jC_{1123} & C_{113\alpha}n_\alpha+p_jC_{1133} \\ C_{121\alpha}n_\alpha+p_jC_{1213} & C_{122\alpha}n_\alpha+p_jC_{1223} & C_{123\alpha}n_\alpha+p_jC_{1233} \\ C_{221\alpha}n_\alpha+p_jC_{2213} & C_{222g\alpha}n_\alpha+p_jC_{2223} & C_{223\alpha}n_\alpha+p_jC_{2233} \end{bmatrix}. \tag{A5}$$

Assume that p_j, $\mathbf{a}_j$, and $\mathbf{b}_j$ $(j=1,2,...,6)$ are the eigenvalues and the associated eigenvectors, we then can order them as

$$\mathrm{Im}\,p_j>0, \quad p_{j+3}=\overline{p_j}, \quad \mathbf{a}_{j+3}=\overline{\mathbf{a}_j}, \quad \mathbf{b}_{j+3}=\overline{\mathbf{b}_j},\mathbf{c}_{j+3}=\overline{\mathbf{c}_j}, \quad (j=1,2,3), \tag{A6}$$

$$\mathbf{A}=[\mathbf{a}_1,\mathbf{a}_2,\mathbf{a}_3], \quad \mathbf{B}=[\mathbf{b}_1,\mathbf{b}_2,\mathbf{b}_3], \quad \mathbf{C}=[\mathbf{c}_1,\mathbf{c}_2,\mathbf{c}_3],$$

where Im stands for the imaginary part and the overbar denotes the complex conjugate. It is further assumed that p_j is distinct and the eigenvectors $\mathbf{a}_j$ and $\mathbf{b}_j$ satisfy the following normalization relation

$$\mathbf{b}_i^T\mathbf{a}_j+\mathbf{a}_i^T\mathbf{b}_j=\delta_{ij}, \tag{A7}$$

with δ_{ij} being the Kronecker delta.

Let us now denote by $\mathbf{U}^\infty(\mathbf{x};\mathbf{y})$ the full-space Green's function tensor[23] with its row and column indices corresponding to the displacement components and point-force directions, respectively, the half-space Green's displacement tensor, with its components bearing the same physical meaning as the full-space one, can then be written in a concise form as[21,24]

$$\mathbf{U}(\mathbf{x};\mathbf{y})=\mathbf{U}^\infty(\mathbf{x};\mathbf{y})+\frac{1}{2\pi^2}\int_0^\pi \overline{\mathbf{A}}\mathbf{G}_1\mathbf{A}^T d\theta, \tag{A8}$$

where (thereafter, the indices i and j take the range from 1 to 3)

$$(\mathbf{G}_1)_{ij}=\frac{(\overline{\mathbf{B}}^{-1}\mathbf{B})_{ij}}{-\overline{p}_i x_3+p_j y_3-[(x_1-y_1)\cos\theta+(x_2-y_2)\sin\theta]}. \tag{A9}$$

Similarly, let $\mathbf{T}^\infty(\mathbf{x};\mathbf{y})$ and $\mathbf{S}^\infty(\mathbf{x};\mathbf{y})$ be the full-space Green's stress tensor,[23] with their components (or the row indices) being defined as

$$\begin{aligned}(\mathbf{T}^\infty)|_{\text{row}}&=(\sigma_{31},\sigma_{32},\sigma_{33})^T,\\ (\mathbf{S}^\infty)|_{\text{row}}&=(\sigma_{11},\sigma_{12},\sigma_{22})^T,\end{aligned} \tag{A10}$$

and their column indices for the point-force directions. Then, the full-space and half space Green's stress tenors can be derived as[21,24]

$$\begin{aligned}\mathbf{T}(\mathbf{x};\mathbf{y})&=\mathbf{T}^\infty(\mathbf{x};\mathbf{y})+\frac{1}{2\pi^2}\int_0^\pi \overline{\mathbf{B}}\mathbf{G}_2\mathbf{A}^T d\theta,\\ \mathbf{S}(\mathbf{x};\mathbf{y})&=\mathbf{S}^\infty(\mathbf{x};\mathbf{y})+\frac{1}{2\pi^2}\int_0^\pi \overline{\mathbf{C}}\mathbf{G}_2\mathbf{A}^T d\theta.\end{aligned} \tag{A11}$$

In Eq. (A11),

$$(\mathbf{G}_2)_{ij}=\frac{(\overline{\mathbf{B}}^{-1}\mathbf{B})_{ij}}{\{-\overline{p}_i x_3+p_j y_3-[(x_1-y_1)\cos\theta+(x_2-y_2)\sin\theta]\}^2}. \tag{A12}$$

Derivatives of the Green's displacement tensor with respect to the source point (y_1,y_2,y_3) can be easily carried out and the results are

$$\frac{\partial\mathbf{U}(\mathbf{x};\mathbf{y})}{\partial y_j}=\frac{\partial\mathbf{U}^\infty(\mathbf{x};\mathbf{y})}{\partial y_j}-\frac{1}{2\pi^2}\int_0^\pi \overline{\mathbf{A}}\mathbf{G}_2\langle g_j\rangle\mathbf{A}^T d\theta, \tag{A13}$$

where

$$\begin{aligned}\langle g_1\rangle&=\text{diag}[\cos\theta,\cos\theta,\cos\theta],\\ \langle g_2\rangle&=\text{diag}[\sin\theta,\sin\theta,\sin\theta],\\ \langle g_3\rangle&=\text{diag}[p_1,\quad p_2,\quad p_3].\end{aligned} \tag{A14}$$

Similarly, the derivatives of the Green's stress tensors with respect to the source point (y_1,y_2,y_3) are

$$\begin{aligned}\frac{\partial\mathbf{T}(\mathbf{x};\mathbf{y})}{\partial y_j}&=\frac{\partial\mathbf{T}^\infty(\mathbf{x};\mathbf{y})}{\partial y_j}-\frac{1}{2\pi^2}\int_0^\pi \overline{\mathbf{B}}\mathbf{G}_3\langle g_j\rangle\mathbf{A}^T d\theta,\\ \frac{\partial\mathbf{S}(\mathbf{x};\mathbf{y})}{\partial y_j}&=\frac{\partial\mathbf{S}^\infty(\mathbf{x};\mathbf{y})}{\partial y_j}-\frac{1}{2\pi^2}\int_0^\infty \overline{\mathbf{C}}\mathbf{G}_3\langle g_j\rangle\mathbf{A}^T d\theta,\end{aligned} \tag{A15}$$

where

$$(\mathbf{G}_3)_{ij}=\frac{(\overline{\mathbf{B}}^{-1}\mathbf{B})_{ij}}{\{-\overline{p}_i x_3+p_j y_3-[(x_1-y_1)\cos\theta+(x_2-y_2)\sin\theta]\}^3}. \tag{A16}$$

Equations (A8), (A11), (A13), and (A15) are the complete Green's functions including displacement, stress, and their derivatives with respect to the source coordinates in a traction-free anisotropic and linearly elastic half-space, namely, the generalized Mindlin solution in an anisotropic and elastic half-space.

[1] D. Bimberg, M. Grundmann, and N. N. Ledentsov, *Quantum Dot Heterostructures* (Wiley, New York, 1998).
[2] M. Grundmann, O. Stier, and D. Bimberg, Phys. Rev. B **52**, 11969 (1995).
[3] T. Benabbas, P. Francois, Y. Androussi, and A. Lefebvre, J. Appl. Phys. **80**, 2763 (1996).
[4] S. Kret, T. Benabbas, C. Delamarre, Y. Androussi, A. Dubon, J. Y. Laval, and A. Lefebvre, J. Appl. Phys. **86**, 1988 (1999).
[5] C. Q. Ru, J. Appl. Mech. **66**, 315 (1999).
[6] D. A. Faux and G. S. Pearson, Phys. Rev. B **62**, R4798 (2000).
[7] J. H. Davies, J. Appl. Phys. **84**, 1358 (1998).
[8] J. H. Davies, Appl. Phys. Lett. **75**, 4142 (1999).
[9] A. D. Andreev, J. R. Downes, D. A. Faux, and E. P. O'Reilly, J. Appl. Phys. **86**, 297 (1999).
[10] G. S. Pearson and D. A. Faux, J. Appl. Phys. **88**, 730 (2000).
[11] E. Kroner, Z. Phys. **136**, 402 (1953).
[12] R. A. Masumura and G. Sines, J. Appl. Phys. **41**, 3930 (1970).
[13] C. S. Chang and Y. Chang, J. Appl. Mech. **62**, 573 (1995).
[14] L. J. Gray, D. Ghosh, and T. Kaplan, Computational Mech. **17**, 255 (1996).
[15] R. D. Mindlin, Physics (N.Y.) **7**, 195 (1936).
[16] T. Mura, *Micromechanics of Defects in Solids* (Martinus Nijhoff, Boston, 1987).
[17] Y. C. Pan and T. W. Chou, Int. J. Eng. Sci. **17**, 545 (1979).
[18] H. Y. Yu and S. C. Sanday, Proc. R. Soc. London, Ser. A **434**, 503 (1991).
[19] A. E. Romanov, G. E. Beltz, W. T. Fischer, P. M. Petroff, and J. S. Speck, J. Appl. Phys. **89**, 4523 (2001).
[20] V. Holy, G. Springholz, M. Pinczolits, and G. Bauer, Phys. Rev. Lett. **83**, 356 (1999).
[21] E. Pan and F. G. Yuan, Int. J. Solids Struct. **37**, 5329 (2000).
[22] T. C. T. Ting, *Anisotropic Elasticity* (Oxford University, Oxford, 1996).
[23] F. Tonon, E. Pan, and B. Amadei, Comput. Struct. **79**, 469 (2001).
[24] E. Pan, J. Appl. Mech. (submitted).
[25] E. Pan, Acta Mech. **87**, 105 (1991).
[26] E. Pan and B. Amadei, Appl. Math. Mod. **20**, 114 (1996).
[27] E. Pan, B. Yang, G. Cai, and F. G. Yuan, Eng. Anal. Boundary Elem. **25**, 31 (2001).
[28] M. P. C. M. Krijn, Semicond. Sci. Technol. **6**, 27 (1991).
[29] S. Adachi, J. Appl. Phys. **58**, R1 (1985).
[30] T. J. Gosling and J. R. Willis, J. Appl. Phys. **77**, 5601 (1995).